

## Article

# Effects of Climate Change on the Moisture Performance of Tallwood Building Envelope

Maurice Defo \* and Michael A. Lacasse

National Research Council Canada, 1200 Montreal Road, Ottawa, ON K1A 0R6, Canada;  
michael.lacasse@nrc-cnrc.gc.ca

\* Correspondence: maurice.defo@nrc-cnrc.gc.ca

**Abstract:** The objective of this study was to assess the potential effects of climate change on the moisture performance and durability of massive timber walls on the basis of results derived from hygrothermal simulations. One-dimensional simulations were run using DELPHIN 5.9.4 for 31 consecutive years of the 15 realizations of the modeled historical (1986–2016) and future (2062–2092) climates of five cities located across Canada. For all cities, water penetration in the wall assembly was assumed to be 1% wind-driven rain, and the air changes per hour in the drainage cavity was assumed to be 10. The mold growth index on the outer layer of the cross-laminated timber panel was used to compare the moisture performance for the historical and future periods. The simulation results showed that the risk of mold growth would increase in all the cities considered. However, the relative change varied from city to city. In the cities of Ottawa, Calgary and Winnipeg, the relative change in the mold growth index was higher than in the cities of Vancouver and St. John's. For Vancouver and St. John's, and under the assumptions used for these simulations, the risk was already higher under the historical period. This means that the mass timber walls in these two cities could not withstand a water penetration rate of 1% wind-driven rain, as used in the simulations, with a drainage cavity of 19 mm and an air changes per hour value of 10. Additional wall designs will be explored in respect to the moisture performance, and the results of these studies will be reported in a future publication.



**Citation:** Defo, M.; Lacasse, M.A. Effects of Climate Change on the Moisture Performance of Tallwood Building Envelope. *Buildings* **2021**, *11*, 35. <https://doi.org/10.3390/buildings11020035>

Received: 10 December 2020

Accepted: 12 January 2021

Published: 20 January 2021

**Publisher's Note:** MDPI stays neutral with regard to jurisdictional claims in published maps and institutional affiliations.



**Copyright:** © 2021 by the authors. Licensee MDPI, Basel, Switzerland. This article is an open access article distributed under the terms and conditions of the Creative Commons Attribution (CC BY) license (<https://creativecommons.org/licenses/by/4.0/>).

## 1. Introduction

Tall wood buildings have been and are being constructed in many jurisdictions across Canada (e.g., the Brock Commons tall wood building at the University of British Columbia, Vancouver and the Origine tall wood building in Quebec City). The wall assemblies are designed to ensure durability in the presence of moisture, energy efficiency, fire safety and noise control. In cold, heating-dominated climate zones, the use of exterior insulation is the preferred thermal design approach [1,2]. From exterior to interior, massive timber wall assemblies are comprised of cladding, a drainage cavity, insulation, an air barrier and water-resistive barrier, and the cross-laminated timber (CLT) panel. The CLT panel is encapsulated in drywall for fire safety, but where it is permitted, it can be left exposed. The use of vapor-permeable insulation is recommended to allow outward drying of the CLT if it is initially wetted or if there is water penetration due to deficiencies. There is no need for a vapor barrier at the interior of the assembly, as is the practice for wood frame construction, since the CLT panel provides sufficient outward vapor resistance. The material and thickness of the insulation depend on the climate zone in which the building is located.

Tall buildings are subjected to increased wind and rain loads, given the increase in building height compared with low-rise constructions. This prolongs the exposure

of building enclosures to wind-driven rain and wind loads. It also increases the risk of water entry to the wall and thus the premature deterioration of wood-based wall and roof assemblies.

There is sufficient evidence that the climate has been warming globally, thereby causing more frequent, intense and extreme climate events such as heat waves, droughts, wildfires, snow and ice storms and flooding, as well as wind and hailstorms [3]. These changes to the climate will have significant effects on building infrastructures and communities, particularly the durability of building materials, as well as the comfort and health of building occupants [4]. These effects should be assessed in order to find appropriate solutions. Building energy simulations and hygrothermal simulations of wall assemblies are typically used to understand the effects of climate loads for the purposes of determining the energy performance of buildings and the risk to deterioration that may occur from the presence of mold or wood rot on assembly components.

A substantial amount of work has been done on the impact of climate change on the thermal performance of buildings [5–12]. The general observation is that there will likely be a reduction in heating demand and an increase in cooling demand in the future.

Other studies have investigated the impacts of climate change on the moisture durability of wall assemblies [13–21]. Grossi et al. [13] found that much of temperate Europe will see a significantly reduced incidence of freezing in the future, which means that the porous stone typically used in the monuments of temperate areas may be less vulnerable to frost damage in the future. Nijland et al. [14] evaluated possible trends and tendencies arising from changes of climate parameters in the future on the durability of building materials in the Netherlands, based upon four scenarios of climate change. They pointed out that the actions of individual climate parameters may strengthen each other, such as a higher temperature combined with higher precipitation, or may result in effects contrary to what might be expected, such as the combination of higher precipitation combined with only a slight decrease in the number of frost-thaw cycles. However, they concluded that damage processes affecting building materials, such as salt damage, rising dampness and biodeterioration, will intensify in the future.

Nick et al. [15] investigated the hygrothermal performance of ventilated attics in respect to possible climate change in Sweden. The results pointed to an increase of moisture problems in attics in the future. Different emissions scenarios did not influence the risk of mold growth inside the attic due to compensating changes in different variables. Assessing the future performance of the four attics showed that the safe solution was to ventilate the attic mechanically. The prospective impacts of climate change on wind-driven rain (WDR) loads were investigated, and the resulting hygrothermal performance was derived through simulation of a common vertical wall construction when subjected to the climatic conditions of Gothenburg, Sweden [16]. The importance of three uncertainty factors of the climate data were investigated and included uncertainties from global climate models, emissions scenarios and spatial resolutions. The consistency of the results was examined by modeling walls with different materials and sizes, as well as using two different mathematical approaches for WDR deposition on the wall. The sensitivity of the simulations to wind data was assessed using a synthetic climate with solely wind data. According to the results, it is anticipated that in the future, higher amounts of moisture will accumulate in walls. Climate uncertainties can cause variations of up to 13% in the calculated 30 year average water content of the wall assemblies and 28% in its standard deviation. Using solely wind data can augment uncertainties by up to 10% in WDR calculations. However, it is possible to neglect changes in future wind data. Nick [17] used synthesized representative weather data of a future climate to undertake impact assessments of the energy usage efficiency of buildings in climate change conditions via simulation. In a similar manner, this approach was extended to the application of corresponding weather data sets for the hygrothermal simulation of buildings, specifically a prefabricated wood frame wall. To investigate the importance of considering moisture and rain conditions when creating representative weather files, two additional groups of weather data were synthesized based

on the distribution of the equivalent temperature and rain. The moisture content, relative humidity, temperature and mold growth rate were calculated in the facade and insulation layers of the wall for several weather data sets. The results showed that the synthesized weather data based on the dry bulb temperature predicted the hygrothermal conditions inside the wall very similarly to the original regional climate model (RCM) weather data, and there is no considerable advantage in using the other two weather data groups.

Sehzadeh and Ge [18] assessed the impact of future climates in the Montréal region on the durability of typical Canadian residential wall assemblies retrofitted to PassiveHaus configurations. The assessment considered current climatic conditions (2015), as well as the climatic conditions of 2020, 2050 and 2080. The durability performance was evaluated in terms of the frost damage risk to brick masonry cladding and the risk of biodegradation of the plywood sheathing within the wall assembly through simulations performed with the WUFI Pro simulation program. The future weather files were generated based on weather data recorded at the Montréal International Airport weather station and a HadCM3 general circulation model, based on the A2 emission scenario as provided by the Intergovernmental Panel on Climate Change. The results from this study indicated that upgrading wall assemblies to the PassiveHaus recommended level would increase the risk to frost damage of bricks, whereas this risk would diminish under 2080 climatic conditions. While the decay risk of the plywood sheathing would decrease, the mold growth risk, defined by *RHT* index (Equation (1)), would increase in future climates. Under future climates, the mold growth risk of the plywood, defined by the mold growth index, would exist only when rain leakage is introduced and would likely decrease for a double-stud wall assembly.

$$RHT = \sum_{k=1}^{k=8760 \text{ hours}} (T - 5)(RH - 80) \quad (1)$$

where  $T$  is the temperature in °C and  $RH$  is the relative humidity in %.

Melin et al. [19] used a simplified hygrothermal model and WUFI Pro to simulate climate-induced damage to heritage objects. Both methods showed that the mean relative humidity inside wood was rather constant, but the minimum and maximum relative humidity varied with the predicted scenario and the type of building used for the simulation.

Vandemeulebroucke et al. [20] used the Canadian initial-condition ensemble RCM4 LE data to assess the impact of climate change on a brick-clad wood-stud wall assembly and a historical solid masonry wall before and after retrofitting for the city of Ottawa. The aim of the study was to evaluate (1) whether the ensemble can be represented by one smaller reduced ensemble for different studies and (2) the potential of using climate-based indices to predict this reduced ensemble. Furthermore, the uncertainty of the ensemble was analyzed, as well as the climate change signal of the damage functions. It was found that the application of a climate ensemble was highly valuable for hygrothermal modeling, as it was able to account for the high uncertainty of climate change data. To maintain the level of information, it was recommended to perform HAM simulations using the entire ensemble. However, there was potential to select a reduced ensemble to represent the spread of the climate change signal.

Most of the studies reported in the literature on the impact of climate change on wall assemblies did not address the specific cases of mass timber buildings. As stated in [19], the hygrothermal response of a wall to climate change depends on the climate scenario and the type of building. Chang et al. [21] did report a study on the impact of climate change on CLT wall assemblies in different climate zones in South Korea. However, their study was limited to only three consecutive years of an observed climate and cannot be exploited when considering long-term change in a climate. Therefore, there is a need to assess the impact of climate change on the moisture performance of tall wood buildings.

The objective of this preliminary work is to evaluate the effects of climate change on the hygrothermal performance and durability of massive timber products used in tall wood building envelopes in five different climate zones across Canada. This will provide

a basis for an ongoing and broader study on the impacts of climate change and extreme events on tall wood buildings across Canada to provide a suitable basis for assuring the durable and climate-resilient design for these structures.

## 2. Methods

The approach described in the *Guideline on Design for Durability of Building Envelopes* [22] was used to assess the hygrothermal performance of massive timber walls under historical and future projected climate loads. One-dimensional simulations were performed using DELPHIN v5.9.4. The cities selected for analysis, the wall configuration, the climate data, the simulation parameters and the performance assessment are described in the following sections.

### 2.1. Cities Selected for the Study

Five Canadian cities were selected for this preliminary study: Calgary, Alberta; Ottawa, Ontario; Vancouver, British Columbia; Winnipeg, Manitoba and St. John's, Newfoundland and Labrador. Their locations and current climate design data [23] are shown in Table 1. Ottawa and St. John's are within the same climate zone, but the moisture index (MI) and driving rain wind pressure (DRWP) are higher in St. John's than in Ottawa. In addition, Calgary and Winnipeg are in the same climate zone, but the annual rain is higher in Winnipeg than in Calgary, whereas the DRWP is higher in Calgary than in Winnipeg. Vancouver (a city center) belongs to zone 4, which is warmer than, but has a comparable MI value to, St. John's (heating degree days (HDD) = 2825).

**Table 1.** Location and climate design data of the selected cities.

City (Province)	Lat	Long	TZO	H	CZ	HDD	MI	Rain	DRWP
	(°)	(°)		(m)				(mm)	(Pa)
Vancouver (BC)	49.3	−123.1	−8	40	4	2825	1.44	1325	160
Ottawa (ON)	45.3	−75.4	−5	125	6	4500	0.84	750	160
St. John's (NL)	47.6	−52.7	−4	65	6	4800	1.41	1200	400
Calgary (AB)	51.1	−114.1	−7	1045	7A	5000	0.37	325	220
Winnipeg (MB)	49.9	−97.1	−6	235	7A	5670	0.58	415	180

Note: Lat = latitude; Long = longitude; TZO = time zone; CZ = climate zone; HDD = heating degree days below 18 °C; MI = moisture index; DRWP = driving rain wind pressure, 1/5; H = elevation.

### 2.2. Building and Wall Components

A 13 story (~41 m) tall wood building with a flat roof was chosen for the study. It was intended that the building be located in the city center. Figure 1 shows the typical composition of the massive timber wall considered. It was a non-load-bearing massive timber wall that consisted of (1) an 11 mm fiberboard used as cladding, (2) a drainage cavity of 19 mm, (3) two layers of mineral fiber insulation, (4) a sheathing membrane (spun bonded polyolefin), (5) 3 layer CLT made of spruce, (6) an air cavity (19 mm) and (7) an interior grade gypsum panel with latex primer and one coat of latex paint. For climate zones 4 (Vancouver), 6 (Ottawa and St. John's), and 7A (Calgary and Winnipeg), the minimum thermal resistance value in metric system (RSI value), as recommended by the National Energy Code for Buildings [24], for above-grade opaque walls is 3.18, 4.05, and 4.76 m<sup>2</sup>K/W, respectively. To meet this requirement, two rows of mineral fiber were used as insulation for climate zones 4 and 6 (64 mm), and 7A (89 mm).

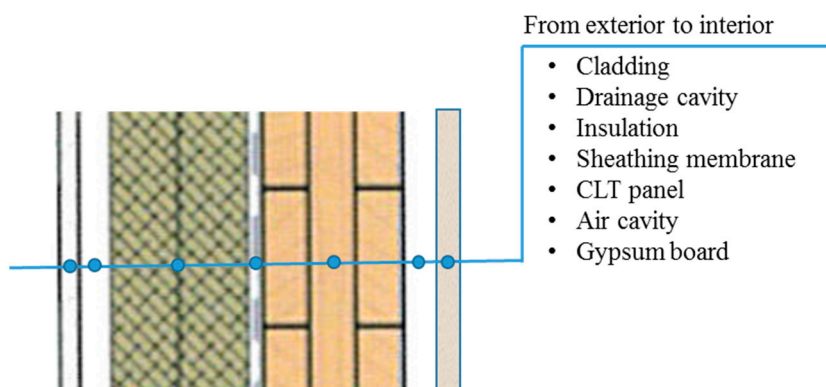


**Figure 1.** Composition of the cross-laminated timber (CLT) wall considered in this study.

The material properties were all obtained from the National Research Council (NRC) hygrothermal material properties database [25], with the exception of the CLT adhesive layer. The CLT adhesive layer (assumed to extend 2 mm deep in the plank) was modeled with the same material properties as spruce, with the exception that the water vapor permeability and liquid water diffusivity were decreased by 50%. In fact, previous studies on the characterization of the hygrothermal properties of CLT have shown that its vapor permeability and moisture diffusivity are substantially reduced in comparison with those of solid wood [26].

### 2.3. Climate Data

The climate data was comprised of modeled hourly time series of the climate variables necessary to undertake hygrothermal simulations for a baseline period spanning from 1986 to 2016 and 31-year-long future periods, when global warming levels of 2 °C and 3.5 °C (with reference to the baseline period) are expected to be reached in the future. The climate datasets were generated to capture the effects of the internal variability of the climate on future climate projections in fifteen hourly realizations that were part of the datasets derived from the large ensemble of climates simulated by the Canadian Regional Climate Model (CanRCM4) version 4, each initialized under a different set of initial conditions in the second generation of Canadian Earth System Model (CanESM2). A detailed description of the procedure used to generate the modeled historical and projected future climate data can be found in [27].

For this study, only the 31 year historical (H: 1986–2016) and future (F: 2062–2092) periods corresponding to a global warming of 3.5 °C were considered. As mentioned above, each timeline was comprised of 15 realizations or runs. Hygrothermal simulations were performed for all 15 runs of each period in order to capture the uncertainties associated with the variability in the climate data. The variability among the different runs of the historical and future periods is illustrated in Figure 2 for the annual average temperature and relative humidity, as well as the annual sum of horizontal rain, in the city of Ottawa. The differences in some of the climate variables between all the runs of the historical and future datasets for the five cities considered are illustrated in Figure 3. The projected changes in some of the climate variables are shown in Table 2. It can be observed from Figure 3 and Table 2 that (1) the annual average temperature will increase significantly between the two timelines in all five cities, (2) the relative humidity will slightly increase in all five cities, (3) the average annual wind speed will decrease in all five cities and (4) the annual rain will increase in all five cities, but at different rates. Although the relative humidity will only slightly increase in the future, the partial pressure of water vapor in the air will significantly increase due to the significant increase in temperature. As illustrated by the change in the interquartile range (Table 2), the uncertainties in the future climate variables were higher than those of the baseline period. Therefore, it was necessary to consider all the runs in order to address uncertainties in the hygrothermal responses.

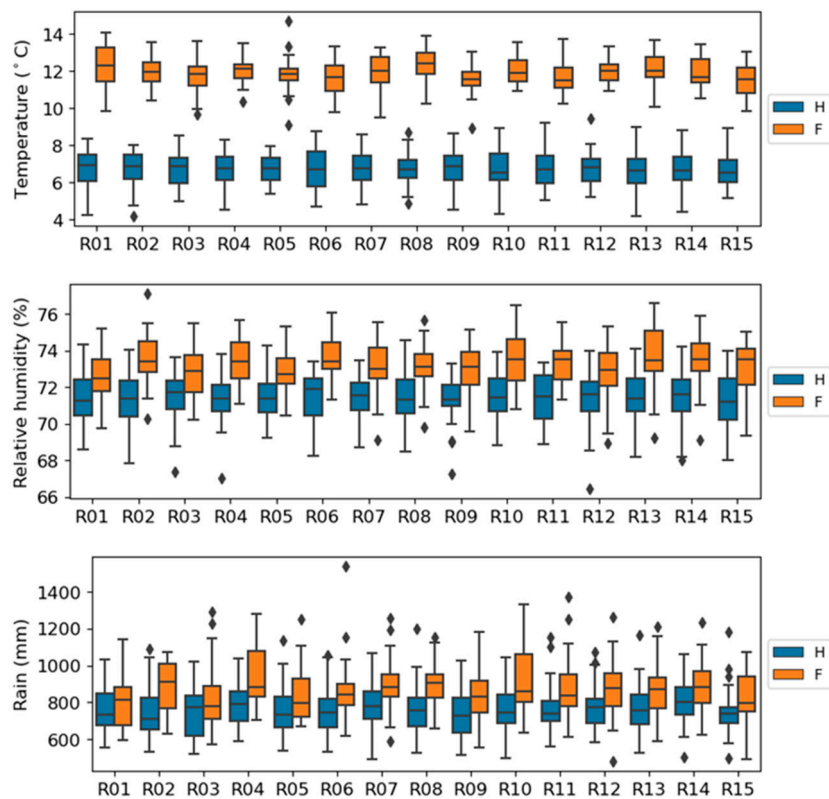


**Figure 2.** Boxplots of the annual average temperature and relative humidity, as well as the annual sum of horizontal rain for runs R01–R15 of the historical (H) and future (F) time periods in the city of Ottawa. Each run comprises 31 consecutive years.

#### 2.4. Hygrothermal Simulations

Simulations were run using the DELPHIN heat, air and moisture simulation tool (version 5.9.4) developed and maintained by the Institute for Building Climatology, Faculty of Architecture, Technical University of Dresden, Germany [28]. It has been successfully validated with HAMSTAD Benchmarks 1–5 [29] and with experimental data [30–33].

To avoid uncertainties related to the selection of moisture reference years, the simulations were performed for all 31 consecutive years of each of the 15 runs with no conditioning years. Only a one-dimensional horizontal configuration of the wall was analyzed, as indicated in Figure 1. The use of a one-dimensional hygrothermal simulation model was deemed sufficient to capture the relative effects of climate change to the moisture performance of the walls.

Using the wind-driven rain rose, the wall orientation was selected as the direction in which the highest quantity of wind-driven rain (WDR) occurred for all the combined years of all the runs in each time period. For both the historical and future timelines, this was found to be 202.5, 135, 337.5, 180 and 22.5° from north for Ottawa, Vancouver, Calgary, St. John's and Winnipeg, respectively.

For the type of building considered in this study, (i.e., a tall building with a flat roof located in a city center), the intensity of rain deposition was higher at the top and edges of the wall, in accordance with the studies by Straube and Burnett [34]. Therefore, only the top area of the building was considered. The amount of rainwater impinging on the building façades was determined based on ASHRAE Standard 160 [35], assuming an exposure factor of 1.5 (height > 20 m) and a deposition rate of 1.0 (wall subject to runoff). The moisture source was determined by assuming water entry beyond the cladding, and that it found its way through the insulation to reach the sheathing membrane. With uncertainties about the quantity of water that penetrated the structure, 1% WDR was assumed to be

deposited on the exterior surface of the sheathing membrane, as suggested by ASHRAE Standard 160 [35].

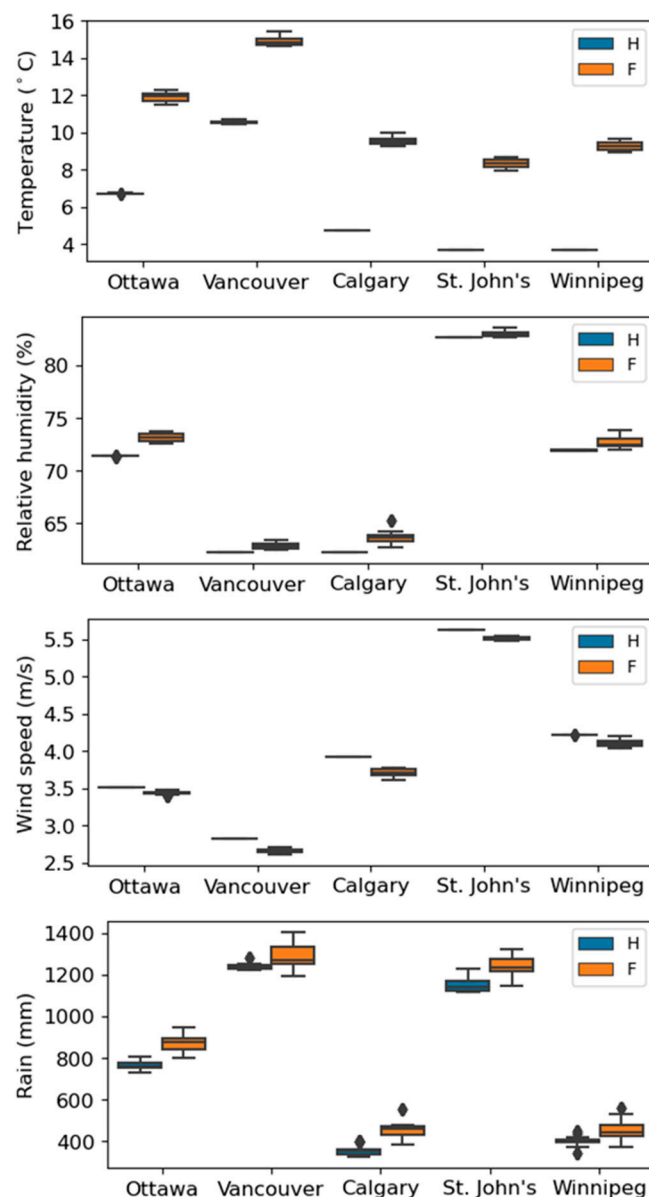


**Figure 3.** Boxplots of run averages of temperature, relative humidity, wind speed, and horizontal rain for the historical (H) and future (F) time periods in the cities of Ottawa, Vancouver, Calgary, St. John's and Winnipeg.

**Table 2.** Projected changes of some of the climate variables under a global warming scenario of 3.5 °C (F: 2062–2092) in comparison with the reference period (H: 1986–2016).

City	Statistic	Temperature			Rain			Relative Humidity			Wind Speed			Global Radiation		
		H	F	% Change	H	F	% Change	H	F	% Change	H	F	% Change	H	F	% Change
		(°C)			(mm)			(%)			(m/s)			(MW/m <sup>2</sup> )		
Ottawa	Minimum	6.7	11.5	71	731	798	9	71.3	72.6	2	3.5	3.4	-3	4.7	4.6	-0.8
	Median	<b>6.7</b>	<b>11.9</b>	<b>78</b>	<b>762</b>	<b>874</b>	<b>15</b>	<b>71.4</b>	<b>73.2</b>	<b>3</b>	<b>3.5</b>	<b>3.4</b>	<b>-2</b>	<b>4.7</b>	<b>4.7</b>	<b>-1.0</b>
	Maximum	6.7	12.3	83	807	945	17	71.4	73.7	3	3.5	3.5	-1	4.8	4.8	-0.1
	IQR <sup>1</sup>	0.0	0.3	6611	20	45	122	0.0	0.6	6481	0.0	0.0	994	0.1	0.1	35.9
Vancouver	Minimum	10.5	14.6	40	1224	1192	-3	62.3	62.5	0	2.8	2.6	-8	3.7	3.8	2.7
	Median	<b>10.6</b>	<b>14.9</b>	<b>41</b>	<b>1243</b>	<b>1272</b>	<b>2</b>	<b>62.3</b>	<b>62.8</b>	<b>1</b>	<b>2.8</b>	<b>2.7</b>	<b>-6</b>	<b>4.0</b>	<b>4.0</b>	<b>1.8</b>
	Maximum	10.7	15.4	44	1282	1406	10	62.3	63.4	2	2.8	2.7	-4	4.1	4.3	3.5
	IQR	0.1	0.3	167	13	73	481	0.0	0.4	3311	0.0	0.0	9530	0.2	0.2	25.2
Calgary	Minimum	4.7	9.3	95	325	383	18	62.3	62.7	1	3.9	3.6	-8	4.8	4.6	-3.8
	Median	<b>4.7</b>	<b>9.5</b>	<b>101</b>	<b>352</b>	<b>461</b>	<b>31</b>	<b>62.3</b>	<b>63.7</b>	<b>2</b>	<b>3.9</b>	<b>3.7</b>	<b>-6</b>	<b>4.9</b>	<b>4.9</b>	<b>-0.4</b>
	Maximum	4.8	10.0	110	402	552	37	62.3	65.3	5	3.9	3.8	-4	5.1	5.0	-2.2
	IQR	0.0	0.3	5007	19	32	64	0.0	0.5	5428	0.0	0.1	4768	0.1	0.1	8.7
St. John's	Minimum	3.7	7.9	116	1114	1147	3	82.7	82.7	0	5.6	5.5	-3	3.7	3.8	1.3
	Median	<b>3.7</b>	<b>8.3</b>	<b>128</b>	<b>1139</b>	<b>1237</b>	<b>9</b>	<b>82.7</b>	<b>82.9</b>	<b>0</b>	<b>5.6</b>	<b>5.5</b>	<b>-2</b>	<b>3.9</b>	<b>4.0</b>	<b>2.8</b>
	Maximum	3.7	8.7	137	1230	1321	7	82.7	83.6	1	5.6	5.5	-1	4.0	4.1	3.3
	IQR	0.0	0.4	28430	31	53	73	0.0	0.3	3917	0.0	0.0	931	0.0	0.1	153.5
Winnipeg	Minimum	3.7	9.0	145	344	372	8	71.9	72.0	0	4.2	4.0	-4	4.6	4.4	-3.3
	Median	<b>3.7</b>	<b>9.3</b>	<b>152</b>	<b>399</b>	<b>443</b>	<b>11</b>	<b>71.9</b>	<b>72.5</b>	<b>1</b>	<b>4.2</b>	<b>4.1</b>	<b>-3</b>	<b>4.6</b>	<b>4.5</b>	<b>-2.5</b>
	Maximum	3.7	9.7	163	447	559	25	72.0	73.9	3	4.2	4.2	-1	4.7	4.6	-2.6
	IQR	0.0	0.3	8371	11	51	362	0.0	0.7	5556	0.0	0.1	3788	0.0	0.1	23.7

<sup>1</sup> IQR = interquartile range.

The initial conditions for the relative humidity (RH) and temperature (T) for all components were set to 50% and 21 °C, respectively. The indoor T and RH were kept constant at 21 °C and 50%, respectively, assuming that the building was equipped with air conditioning and dehumidification. Referring to the ISO 6946 Standard [36], the indoor convective heat transfer coefficient was set to 2.5 W/m<sup>2</sup>K, and the outdoor convective heat transfer coefficient was calculated using Equation (2):

$$\alpha_{ce} = 4 + 4V \quad (2)$$

where  $\alpha_{ce}$  is the outdoor convective heat transfer coefficient in W/m<sup>2</sup> K and V is the wind speed, corrected for the height of the building (m/s).

The outdoor and indoor convective vapor transfer coefficients were calculated using the convective heat transfer and the Lewis number [37]. The indoor radiative heat transfer coefficient was set to 5.5 W/m<sup>2</sup>K [36], whereas the longwave exchange between the cladding surface and the environment was explicitly calculated assuming a longwave emissivity of 0.9 for the surface and the surrounding ground and 1.0 for the sky. The ground surface temperature and albedo were set to the air temperature and 0.2, respectively. The shortwave absorption coefficient of the cladding was set at 0.6, assuming a red-colored surface.

The air was assumed to still be in the air cavity between the drywall and the CLT, but air transfer in the drainage cavity was expected, having an air change per hour (ACH) of 10 in all cities.

### 2.5. Moisture Performance Assessment

The outer layer (0.5 mm) of the CLT was used as the critical location from which to compare the effects of climate change on the moisture performance of the wall, using the mold growth index (MI) as the indicator. As recommended by ASHRAE Standard 160 [35], the empirical model used for calculating the MI was the one developed by Hukka and Viitanen [38] and Ojanen, Viitanen, Peuhkuri and Lahdesmaki et al. [39]. The MI profiles over time, the maximum and mean MI, as well as the percentage of time when the MI remained above 3 (the level at which mold is visible) were used for comparison.

## 3. Results and Discussion

Figure 4 shows the median profiles of the mold index obtained under both the historical and future periods in the cities of Ottawa, Vancouver, Calgary, St. John's and Winnipeg. The uncertainty due to internal climate variability (variability of climate variables among different runs) is shown in each case by the shaded area that represents the minimum and maximum of the hourly values obtained for all runs. In the city of Ottawa, the difference between the median mold profiles obtained under the historical and future periods was obvious: the risk of mold growth on the outer layer of CLT will increase in the future. This is in agreement with other studies that suggested the combined increase in T and WDR in certain regions will likely increase the risk of mold growth [14,16,18]. In the cities of Vancouver and St. John's, where the risk of mold growth was already high under the modeled reference climate, the risk of mold growth will remain higher in both cities with less uncertainty in the results (less difference among the runs). In the cities of Calgary and Winnipeg, although the median profile for the future period remained above that of the baseline period, the higher uncertainty in the results and the partial overlapping of the uncertainty bands for both periods made it difficult to draw definitive conclusions.

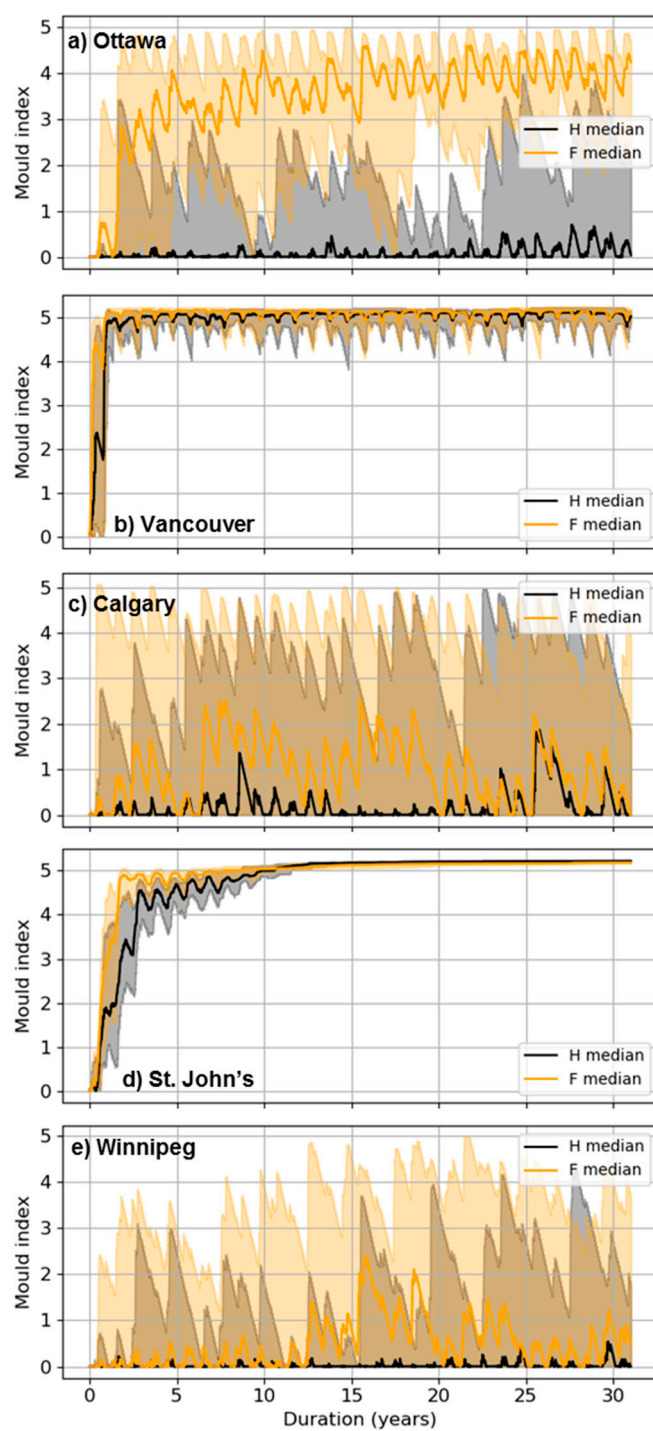


**Figure 4.** Mold index profiles obtained under the historical (H) and future (F) time periods in the city of Ottawa. The error band (minimum and maximum of the hourly run values) represents the uncertainty due to the internal variability of the modeled climate data.

To ease the interpretation of the results, the mean value of the mold index was calculated for each of the 15 runs. Additionally, the maximum value of the mold index for each of the 15 runs was extracted. The results of these two statistics are summarized in Figures 5 and 6 for the distribution of means and maxima of the runs, respectively, and in Table 3 in terms of the projected change of the percentiles (25th, 50th (median), 75th, and 100th) of the means and maxima of the runs. A statistical test was performed to compare the means and maxima of the runs for the historical and future timelines in each

city. First, the normality of the distribution of the mean and maximum values of the runs was verified for each case using Shapiro's test [40]. If they were not normally distributed, a log or square root transformation was tested. Then, the homoscedasticity of the two groups was tested using Barlett's test [41]. When the two assumptions were verified, the Student's *t*-test for two samples was used to compare the two means and maxima. When neither the assumption of normality nor homoscedasticity was still not verified after data transformation, the Mann–Whitney U test [18] was used. All the tests were performed using the SciPy package [42] of Python [43]. Overall, the median values for the means and maxima of the runs under the baseline and future periods were found to be significantly different in all cities ( $p < 0.001$ ). However, the relative changes varied from city to city (Figures 5 and 6 and Table 3).

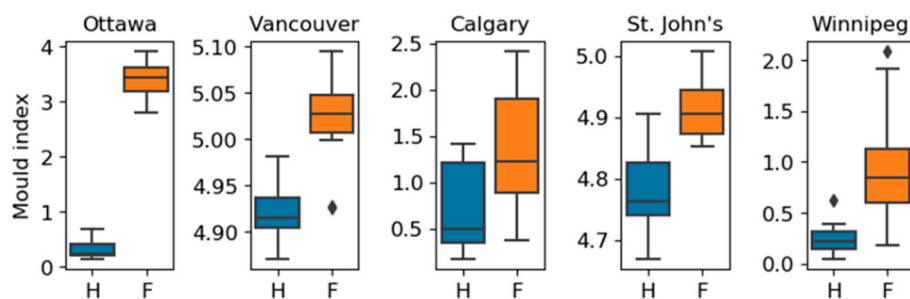


**Figure 5.** Boxplots of the mean mold index obtained per run under the historical (H) and future (F) time periods in the cities of Ottawa, Vancouver, Calgary, St. John's and Winnipeg.

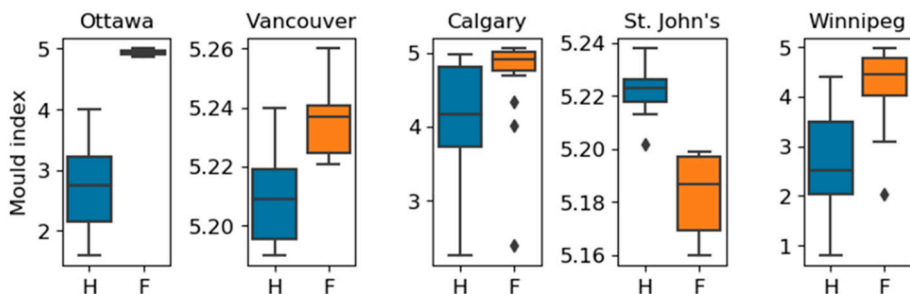


**Figure 6.** Boxplots of the maximum mold index obtained per run under the historical (H) and future (F) time periods in the cities of Ottawa, Vancouver, Calgary, St. John's and Winnipeg.

In the city of Ottawa, all the percentile values of the means and maxima of the runs will increase significantly in the future. The 25th percentile of the means and maxima of the runs will increase by 1518% and 129%, respectively. The median value of the means and maxima of the runs will increase by 1432% and 80%, respectively. Both the 75th percentile and maximum value for the means and maxima of runs will also increase in the future. This significant change in the mold growth index in Ottawa may be explained by the increase in rain (15%), as shown in Table 2. The projected increase in the risk of mold growth in the cities of Calgary and Winnipeg followed the same trend as in the city of Ottawa. However, the increase was not as significant as that in Ottawa. For example, the median value of the mean values of the runs increased by 149% and 290% in Calgary and Winnipeg, respectively, compared with 1432% in Ottawa. The projected increase in rain was 31% in Calgary and 11% in Winnipeg. As such, one would have expected a higher increase in mold growth in Calgary than in Ottawa and a similar increase in Winnipeg as in Ottawa. Table 2 shows a higher projected decrease in the median wind speed (−5.5% in Calgary compared with −2.2% in Ottawa) and global radiation (−0.4% in Calgary compared with −1.0% in Ottawa). The difference in the relative change of the climate variables and their complex interactions may explain the difference in the projected change in mold growth in these cities.

**Table 3.** Projected changes in mold index statistics under a global warming scenario of 3.5 °C (F: 2062–2092) in comparison with the reference period (H: 1986–2016).

City	Statistic	Run Means			Run Maxima			% Time MI > 3		
		H	F	% Change	H	F	% Change	H	F	% Change
Ottawa	25th percentile	0.2	3.2	1518	2.1	4.9	129	0.0	66.1	...
	Median	0.2	3.4	1432	2.7	5.0	80	0.0	75.7	...
	75th percentile	0.4	3.6	773	3.2	5.0	55	0.7	82.6	11,074
	Maximum	0.7	3.9	481	4.0	5.0	25	5.1	92.0	1706
Vancouver	25th percentile	4.9	5.0	2	5.2	5.2	0	97.1	98.1	1
	Median	4.9	5.0	2	5.2	5.2	0	97.3	99.5	2
	75th percentile	4.9	5.0	2	5.2	5.2	0	98.9	99.6	1
	Maximum	5.0	5.1	2	5.2	5.3	0	99.4	99.8	0
Calgary	25th percentile	0.4	0.9	153	3.7	4.8	28	2.1	8.3	286
	Median	0.5	1.2	149	4.2	4.9	17	4.0	17.2	328
	75th percentile	1.2	1.9	57	4.8	5.0	4	15.2	26.5	74
	Maximum	1.4	2.4	70	5.0	5.1	2	23.8	44.6	88
St. John's	25th percentile	4.7	4.9	3	5.2	5.2	0	91.8	95.0	4
	Median	4.8	4.9	3	5.2	5.2	0	94.0	96.9	3
	75th percentile	4.8	4.9	2	5.2	5.2	0	95.1	97.4	2
	Maximum	4.9	5.0	2	5.2	5.2	0	97.5	97.9	0
Winnipeg	25th percentile	0.1	0.6	324	2.0	4.0	97	0.0	4.8	...
	Median	0.2	0.8	290	2.5	4.4	76	0.0	7.6	...
	75th percentile	0.3	1.1	254	3.5	4.8	37	1.3	13.4	946
	Maximum	0.6	2.1	232	4.4	5.0	13	5.1	30.5	499

The trends observed in the cities of Vancouver and St. John's were similar: the projected changes in statistics for the values of the means and maxima of the runs, although significant, were marginal (< 3%). In fact, the moisture loads under the baseline period were already high in these two cities. As a consequence, the mold index value reached its maximum value during the first few years (2 years in Vancouver and 10 years in St. John's) and stayed close to that level for the remaining time. Under the future climate, even if there were an increase in moisture loads, the material cannot absorb water beyond its capacity. In addition, the value of the mold growth index cannot go beyond the maximum for the material, even if the mold growth intensity increases. Nik [17] suggested using the rate of the mold growth index rather than the mold growth index itself to assess the effect of climate change. It should be noted that in St. John's, there was a significant but negligible decrease in the maxima of the runs.

The proportion of the total number of hours to the mold index values was greater than three for each timeline, and the projected changes for various statistics are shown in Table 3. The results were quite similar to those observed for the means and maxima of the runs. The projected changes were higher in Ottawa, Calgary and Winnipeg than in Vancouver and St. John's. For these latter two cities, the mold index was above three most of the time (>90%).

The climate data used for the baseline period was modeled and may not have reflected the actual climate conditions. In order to test what would be the actual response of the wall in the cities of Ottawa, Calgary, Vancouver, Winnipeg and St. John's, simulations were performed using observed data for the baseline period (1986–2016). The results are shown in Figure 7. In general, the median mold index profile of all 15 runs, obtained using the modeled historical climate, agreed well with the observed one, with the exceptions of Vancouver and St. John's. In fact, in Vancouver between years 22 and 27 and in St. John's for the first 3 years, the observed mold index profile fell outside the uncertainty range defined by the minimum and maximum modeled mold index profiles.

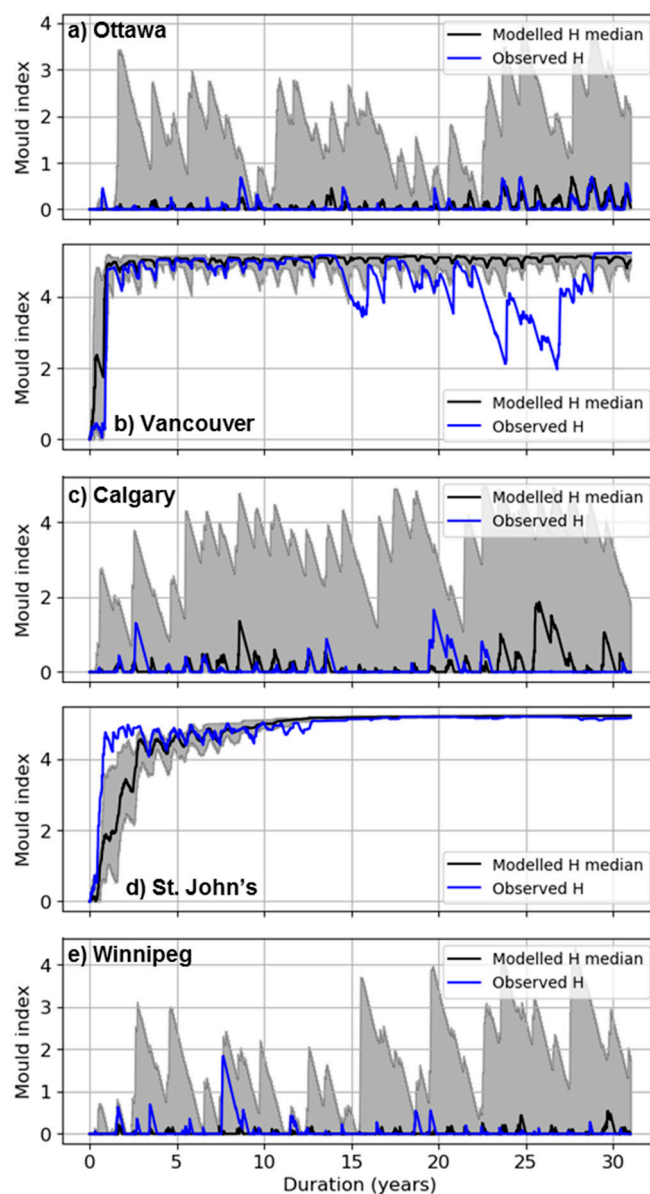


**Figure 7.** Comparison of mold indexes obtained under historical modeled and observed climates in the cities of Ottawa, Vancouver, Calgary, St. John’s and Winnipeg.

These results were obtained by applying 1% WDR as a water source and 10 as the air changes per hour in all five cities considered. In reality, given the difference in wind speed (Table 2 and Figure 3), and therefore the wind pressure in the five cities and between historical and future periods, the water penetration rate should have varied, as shown by prior experimental methods [44,45]. Additionally, the outdoor temperature and wind speed affect the air flow rate in the drainage cavity [46]. In this study, similar values of water penetration and ACH were used in all the cities. They were not meant to represent the real situation, but permit comparison of the moisture performance of CLT walls among different cities and between historical and future climate periods.

#### 4. Conclusions

The objective of this study was to assess the relative effects of climate change on the moisture performance of massive timber walls in five cities having different climate characteristics: Ottawa, Ontario; Vancouver, British Columbia; Calgary, Alberta; Winnipeg, Manitoba and St. John’s, Newfoundland and Labrador. The configuration of the wall

studied was comprised of fiberboard cladding, a drainage cavity, spunbonded polyolefin as a sheathing membrane, mineral fiber insulation, a three-layer CLT panel, an air cavity and a gypsum board. The thickness of the insulation layer was chosen to meet the energy requirement for each city. A tall wood building of a height of 41 m was considered. One-dimensional simulations were run using DELPHIN 5.9.4 for 31 consecutive years of the 15 realizations of modeled historical (1986–2016) and future (2062–2092) climates. The wall orientation receiving the highest quantity of wind-driven rain for all the combined years of all the runs in each time period was selected for simulations in each city. The water penetration in the wall assembly was assumed to be 1% wind-driven rain. A value of 10 air changes per hour was assumed for all the cases analyzed. The temperature and relative humidity of the outer layer of the CLT panel were used to compute the mold growth index.

The simulation results showed that the risk of mold growth would increase in all the cities considered due to an increase in rain loads. However, the relative changes of the median values of the run means between the baseline and future periods varied from city to city. In the city of Ottawa, the relative change of the median value of the run means was about 1432% (from 0.2 under the baseline period to 3.2 under the future period). The projected increase in the risk of mold growth in the cities of Calgary and Winnipeg followed the same trend as in the city of Ottawa. However, the increase was not as high as in Ottawa. The median value of the run means increased by 149% (from 0.5 to 1.2) and 290% (from 0.2 to 0.8) in Calgary and Winnipeg, respectively. Unlike Ottawa, in Calgary and Winnipeg, the projected change in the risk of mold growth was marginal (< 3%) in Vancouver and St. John's. In fact, the risk of mold growth was already high in these two cities under the baseline period. Since the mold growth index cannot go beyond a maximum for a given material, any increase in moisture loads will not be translated directly into an increase in the mold growth index.

The wall assembly considered in this study did not perform well in Vancouver and St. John's under the baseline period. This was confirmed using the observed historical climate. This implies that the mass timber walls located in these two cities, configured with a drainage cavity of 19 mm and having an assumed cavity air change rate of 10 per hour, cannot withstand a water penetration rate of 1% wind-driven rain, as was used in the simulations.

**Author Contributions:** M.D. and M.A.L. designed the study. M.D. performed simulations, analyzed the data, conceived the paper, wrote the first draft and addressed the reviewers and editor comments. M.A.L. revised the first draft. All authors have read and agreed to the published version of the manuscript.

**Funding:** This work was carried out by the National Research Council of Canada with funding from Infrastructure Canada in support of the Pan Canadian Framework on Clean Growth and Climate Change, and further development of the National Building Code of Canada.

**Institutional Review Board Statement:** Not applicable (study not involving humans or animals).

**Informed Consent Statement:** Not applicable (study not involving humans).

**Data Availability Statement:** Climate data used in this study were obtained from Gaur, A.; Lacasse, M.; Armstrong, M. Climate Data to Undertake Hygrothermal and Whole Building Simulations Under Projected Climate Change Influences for 11 Canadian Cities. *Data* **2019**, *4*(2), 72 and are available online at <http://www.mdpi.com/2306-5729/4/2/72/s1>, File: data-498712\_supplementary material.docx. Material properties data were obtained from Kumaran et al. (2002) and are available in: Kumaran, M.K.; Lackey, J.C.; Normandin, N.; Tariku, F.; van Reenen, D. *A Thermal and Moisture Transport Property Database for Common Building and Insulating Materials: Final Report from ASHRAE Research Project 1018-RP*. American Society of Heating, Refrigerating and Air-Conditioning Engineers, Inc.: Atlanta, GA, USA, 2002. Data obtained from simulations in this study are available on request from the corresponding authors.

**Acknowledgments:** The authors would like to thank Abhishek Gaur for providing the climate data. We also acknowledge constructive feedback from two anonymous reviewers and the editor that greatly helped in improving the quality of the manuscript.

**Conflicts of Interest:** The authors declare no conflict of interest.

## References

1. Gagnon, S.; Pirvu, C. *Cross-Laminated Timber*; Special Publication; SP-528E; FPInnovations: Pointe-Claire, QC, Canada, 2011.
2. Karacabeyli, E.; Lum, C. *Technical Guide for the Design and Construction of Tall Wood Buildings in Canada*, 1st ed.; Special Publication, SP-55E; FPInnovations: Pointe-Claire, QC, Canada, 2014.
3. Intergovernmental Panel on Climate Change (IPCC). *AR5 Synthesis Report: Climate Change 2014*; IPCC: Geneva, Switzerland, 2014.
4. Bizikova, L.; Neale, T.; Burton, I. *Canadian Communities' Guidebook for Adaptation to Climate Change*; Environment Canada: Ottawa, ON, Canada, 2009.
5. Aguiar, R.; Oliveira, M.; Gonccedilalves, H. Climate change impacts on the thermal performance of Portuguese buildings. Results of the SIAM study. *Build. Serv. Eng. Res. Technol.* **2002**, *23*, 223–231. [[CrossRef](#)]
6. Gaterell, M.R.; McEvoy, M.E. The impact of climate change uncertainties on the performance of energy efficiency measures applied to dwellings. *Energy Build.* **2005**, *37*, 982–995. [[CrossRef](#)]
7. Zmeureanu, R.; Renaud, G. Estimation of potential impact of climate change on the heating energy use of existing houses. *Energy Policy* **2008**, *36*, 303–310. [[CrossRef](#)]
8. Wang, X.; Chen, D.; Ren, Z. Assessment of climate change impact on residential building heating and cooling energy requirement in Australia. *Build. Environ.* **2010**, *45*, 1663–1682. [[CrossRef](#)]
9. Wan, K.K.; Li, D.H.; Pan, W.; Lam, J.C. Impact of climate change on building energy use in different climate zones and mitigation and adaptation implications. *Appl. Energy* **2012**, *97*, 274–282. [[CrossRef](#)]
10. Chow, D.H.C.; Li, Z.; Darkwa, J. The effectiveness of retrofitting existing public buildings in face of future climate change in the hot summer cold winter region of China. *Energy Build.* **2013**, *57*, 176–186. [[CrossRef](#)]
11. Berger, T.; Amann, C.; Formayer, H.; Korjenic, A.; Pospischal, B.; Neururer, C.; Smutny, R. Impacts of climate change upon cooling and heating energy demand of office buildings in Vienna, Austria. *Energy Build.* **2014**, *80*, 517–530. [[CrossRef](#)]
12. Nematchoua, M.K.; Yvon, A.; Kalameu, O.; Asadi, S.; Choudhary, R.; Reiter, S. Impact of climate change on demands for heating and cooling energy in hospitals: An in-depth case study of six islands located in the Indian Ocean region. *Sustain. Cities Soc.* **2019**, *44*, 629–645. [[CrossRef](#)]
13. Grossi, C.M.; Brimblecombe, P.; Harris, I. Predicting long term freeze–thaw risks on Europe built heritage and archaeological sites in a changing climate. *Sci. Total Environ.* **2007**, *377*, 273–281. [[CrossRef](#)]
14. Nijland, T.G.; Adam, O.C.; Van Hees, R.P.; van Etten, B.D. Evaluation of the effects of expected climate change on the durability of building materials with suggestions for adaptation. *Heron* **2009**, *54*, 37–48.
15. Nik, V.M.; Kalagasisidis, A.S.; Kjellström, E. Assessment of hygrothermal performance and mould growth risk in ventilated attics in respect to possible climate changes in Sweden. *Build. Environ.* **2012**, *55*, 96–109. [[CrossRef](#)]
16. Nik, V.M.; Mundt-Petersen, S.O.; Kalagasisidis, A.S.; De Wilde, P. Future moisture loads for building facades in Sweden: Climate change and wind-driven rain. *Build. Environ.* **2015**, *93*, 362–375. [[CrossRef](#)]
17. Nik, V.M. Application of typical and extreme weather data sets in the hygrothermal simulation of building components for future climate—A case study for a wooden frame wall. *Energy Build.* **2017**, *154*, 30–45. [[CrossRef](#)]
18. Melin, B.C.; Hagentoft, C.E.; Holl, K.; Nik, V.M.; Kilian, R. Simulations of moisture gradients in wood subjected to changes in relative humidity and temperature due to climate change. *Geosciences* **2018**, *8*, 378. [[CrossRef](#)]
19. Sehzadeh, A.; Ge, H. Impact of future climates on the durability of typical residential wall assemblies retrofitted to the PassiveHaus for the Eastern Canada region. *Build. Environ.* **2016**, *97*, 111–125. [[CrossRef](#)]
20. Vandemeulebroucke, I.; Defo, M.; Lacasse, M.A.; Caluwaerts, S.; Van Den Bossche, N. Canadian initial-condition climate ensemble: Hygrothermal simulation on wood-stud and retrofitted historical masonry. *Build. Environ.* **2020**, *187*, 107318. [[CrossRef](#)]
21. Chang, S.J.; Yoo, J.; Wi, S.; Kim, S. Numerical analysis on the hygrothermal behavior of building envelope according to CLT wall assembly considering the hygrothermal-environmental zone in Korea. *Environ. Res.* **2020**, *191*, 110198. [[CrossRef](#)]
22. Lacasse, M.A.; Ge, H.; Hegel, M.; Jutras, R.; Laouadi, A.; Sturgeon, G.; Wells, J. *Guideline on Design for Durability of Building Envelopes*; CRBCPI-Y2-R19; National Research Council Canada: Ottawa, ON, Canada, 2018.
23. NRC. *National Building Code of Canada*; National Research Council of Canada: Ottawa, ON, Canada, 2015.
24. NRC. *National Energy Code of Canada for Buildings*; National Research Council of Canada: Ottawa, ON, Canada, 2017.
25. Kumaran, M.K.; Lackey, J.C.; Normandin, N.; Tariku, F.; van Reenen, D. *A Thermal and Moisture Transport Property Database for Common Building and Insulating Materials: Final Report from ASHRAE Research Project 1018-RP*; American Society of Heating, Refrigerating and Air-Conditioning Engineers, Inc.: Atlanta, GA, USA, 2002.
26. Al Sayegh, G. Hygrothermal Properties of Cross-Laminated Timber and Moisture Response of Wood at High Relative Humidity. Master's Thesis, Carleton University, Ottawa, ON, Canada, 2012.
27. Gaur, A.; Lacasse, M.; Armstrong, M. Climate data to undertake hygrothermal and whole building simulations under projected climate change influences for 11 Canadian cities. *Data* **2019**, *4*, 72. [[CrossRef](#)]
28. DELPHIN. Simulation Program for the Calculation of Coupled Heat, Moisture, Air, Pollutant, and Salt Transport. Available online: <http://bauklimatik-dresden.de/delphin/index.php> (accessed on 30 December 2020).
29. Sontag, L.; Nicolai, A.; Vogelsang, S. *Validierung der Solverimplementierung des Hygrothermischen Simulationsprogramms Delphin*; Institute for Building Climatology: Dresden, Germany, 2013.

30. Langmans, J.; Nicolai, A.; Klein, R.; Roels, S. A quasi-steady state implementation of air convection in a transient heat and moisture building component model. *Build. Environ.* **2012**, *58*, 208–218. [[CrossRef](#)]
31. Vogelsang, S.; Kehl, D.; Ruisinger, U.; Meissner, F. Three-dimensional HAM Transport in Timber Beam Ends—Measurements and Simulation. In Proceedings of the 5th German-Austrian Conference of the International Building Performance Simulation Association, Aachen, Germany, 22–24 September 2014.
32. Hejazi, B.; Sakiyama, N.R.; Frick, J.; Garrecht, H. Hygrothermal Simulations Comparative Study: Assessment of Different Materials Using WUFI and DELPHIN Software. In Proceedings of the 16th IBPSA International Conference, Rome, Italy, 2–4 September 2019.
33. Ruisinger, U.; Kautsch, P. Comparison of hygrothermal 2D-and 3D-simulation results with measurements from a test house. In Proceedings of the 12th Symposium on Building Physics, E3S Web of Conferences 172, Tallinn, Estonia, 6–9 September 2020.
34. Straube, J.F.; Burnett, E.F.P. Simplified prediction of driven rain deposition. In Proceedings of the International building physics conference, Eindhoven, The Netherlands, 18–21 September 2000.
35. American Society of Heating, Refrigerating and Air-Conditioning Engineers, Inc. (ASHRAE). *ASHRAE Standard 160-2016, Criteria for Moisture-Control Design Analysis in Buildings*; ASHRAE: Atlanta, GA, USA, 2016.
36. International Organization for Standardization (ISO). ISO 6946, *Building Components and Building Elements-Thermal Resistance and Thermal Transmittance-Calculation Methods*; ISO: Geneva, Switzerland, 2017.
37. Incropera, F.P.; DeWitt, D.P. *Fundamentals of Heat Andmass Transfer*, 4th ed.; John Wiley and Sons: New York, NY, USA, 1996.
38. Hukka, A.; Viitanen, H. A mathematical model of mould growth on wooden material. *Wood Sci. Technol.* **1999**, *33*, 475–485. [[CrossRef](#)]
39. Ojanen, T.; Viitanen, H.; Peuhkuri, R.; Lähdesmäki, K.; Vinha, J.; Salminen, K. Mold growth modeling of building structures using sensitivity classes of materials. In Proceedings of the Thermal Performance of the Exterior Envelopes of Whole Buildings XI International Conference, Clearwater Beach, FL, USA, 1–5 December 2010.
40. Razali, N.; Wah, Y.B. Power comparisons of Shapiro-Wilk, Kolmogorov-Smirnov, Lilliefors and Anderson-Darling tests. *J. Stat. Modeling Anal.* **2011**, *2*, 21–33.
41. McDonald, J. *Handbook of Biological Statistics*, 3rd ed.; Sparky House Publishing: Baltimore, MD, USA, 2014.
42. Virtanen, P.; Gommers, R.; Oliphant, T.E.; Haberland, M.; Reddy, T.; Cournapeau, D.; Burovski, E.; Peterson, P.; Weckesser, W.; Bright, J.; et al. SciPy 1.0: Fundamental Algorithms for Scientific Computing in Python. *Nat. Methods* **2020**, *17*, 261–272. [[CrossRef](#)] [[PubMed](#)]
43. Van Rossum, G.; Drake, F.L. *Python 3 Reference Manual*; CreateSpace: Scotts Valley, CA, USA, 2009.
44. Saber, H.; Lacasse, M.; Moore, T.; Nicholls, M. *Mid-Rise Wood Constructions: Investigation of Water Penetration through Cladding and Deficiencies, Report to Research Consortium for Wood and Wood-Hybrid Mid-Rise Buildings*; National Research Council: Ottawa, ON, Canada, 2014.
45. Moore, T.; Lacasse, M. Approach to Incorporating Water Entry and Water Loads to Wall Assemblies When Completing Hygrothermal Modelling. In *Building Science and the Physics of Building Enclosure Performance*; Lemieux, D., Keegan, J., Eds.; ASTM International: West Conshohocken, PA, USA, 2020; pp. 157–176.
46. Straube, J.; Finch, G. *Ventilated Wall Claddings: Review, Field Performance, and Hygrothermal Modelling*; Research Report-0906; Building Science Press: San Rafael, CA, USA, 2009.